

Drop Sizes in Liquid Membrane Dispersions

Tatiana Gallego-Lizon[†] and E. Susana Pérez de Ortiz*

Department of Chemical Engineering and Chemical Technology, Imperial College of Science, Technology and Medicine, London SW7 2BY, England

The effect of hydrodynamic conditions and physical properties on the characteristics of an emulsion dispersion in a stirred tank was studied in the presence of mass transfer, in an attempt to identify the parameters for Sauter mean diameter data correlation in emulsion liquid membranes. The organic phase of the water-in-oil emulsion contained the cadmium extractant Cyanex 302 and an emulsion stabilizer, and the dispersion continuous phase was an aqueous solution of phosphoric acid containing cadmium. Variations in emulsion viscosity and interfacial tension were achieved by changing the extractant and surfactant concentrations. The dispersion drop size distribution was measured from photographs taken with a high-speed video camera system attached to an endoscope. It was found that the emulsion physical properties, emulsion swelling, and operating conditions were interrelated in a complex way. However, emulsion swelling seemed to lump together the effect of some of the parameters on globule size, which made possible the development of a simple correlation for the Sauter mean diameter in terms of $We^{-0.6}$, emulsion swelling percentage, and empirical correction factors for emulsion viscosity and dispersed-phase holdup. A modified Rosin–Rammmler probability distribution function fitted well the globule size distribution data.

Introduction

An emulsion liquid membrane (ELM) is a three-liquid-phase configuration consisting of two phases of the same nature (usually aqueous) separated by a third one, called the liquid membrane, immiscible with the other two. A typical system consists of a water-in-oil emulsion, stabilized by addition of a surfactant, dispersed in an aqueous solution in an agitated contactor (Figure 1). The three-phase dispersion obtained in this way can be either a water-in-oil emulsion dispersed in an aqueous phase (W/O/W) or an oil-in-water emulsion dispersed in an oil phase (O/W/O). In either form, ELMs are used as separation processes in which a solute is extracted from the continuous phase into the liquid membrane, and from there into the emulsion droplets, by selective solubilization or by chemical reaction.

The emulsion globule size and the globule size distribution affect the extraction performance of the ELM in the same way as drop size and drop size distribution affect conventional solvent extraction: they determine both the area available to mass transfer and the mass-transfer coefficients. Therefore, knowledge of dispersion characteristics and their dependency on physical properties and hydrodynamic conditions is required in order to predict the extraction performance.

Despite the substantial amount of research on two-phase liquid–liquid dispersions conducted over the last several decades, there are no correlations that can confidently be used to predict the average drop size outside the range of conditions at which they were tested. Mechanistic equations for the prediction of the dispersion drop size are based on the work of Hinze,¹ who proposed that drop breakup resulted from the balance between the disruptive force caused by the

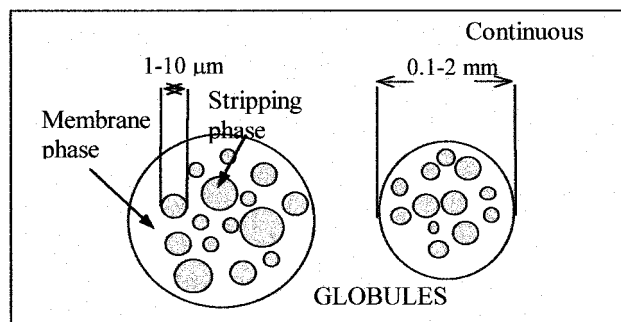


Figure 1. Emulsion liquid membrane.

variation of dynamic pressure on the drop surface and the resistive forces due to interfacial tension and dispersed-phase viscosity. Further work by Shinnar and Church² led to the basic equation for the Sauter mean diameter of noncoalescing, dilute dispersions of low-viscosity liquids, generated in baffled cylindrical tanks:

$$d_{32}/d_1 = C_1 We^{-0.6} \quad (1)$$

$$We = \rho_c N^2 d_1^3 / \sigma \quad (2)$$

where d_{32} is the Sauter mean diameter defined as

$$d_{32} = \frac{\sum n_i d_i^3}{\sum n_i d_i^2} \quad (3)$$

d_1 is the impeller diameter, C_1 is a constant that depends on the tank geometry, and We is the Weber number. Equation 1 is based on Kolmogorov's theory of isotropic turbulence.³ Mechanistic and empirical correction factors have been added to this equation by various investigators in order to account for the density difference between the phases, for the viscosity of the dispersed phase, and for the effect of the dispersed-phase fraction on coalescence when the assumption of

* To whom correspondence should be addressed. E-mail: s.ortiz@ic.ac.uk. Fax: +44 (0)20 7594 5700.

[†] Current address: SmithKline Beecham (Pharmaceuticals), Old Powder Mills, Tonbridge, Kent TN11 9AN, England.

Table 1. Sauter Mean Globule Diameter Correlations for Emulsion Dispersions

reference	correlation	conditions and notes	eq
Kataoka and Nishiki ¹⁰	$d_{32}/d_1 = 0.016[We(\Delta\rho/\rho_2)(\mu_1/\mu_2)]^{-0.375}$	Span 80, no carrier, no solute transfer, no swelling	(4)
	$d_{32}/d_1 = 0.012[We(\Delta\rho/\rho_2)(\mu_1/\mu_2)]^{-0.22}$	Span 80, carrier, solute transfer, swelling	(5)
	$d_{32}/d_1 = 0.066[We(\Delta\rho/\rho_2)(\mu_1/\mu_2)]^{-0.75}$	ECA 4360J, carrier, solute transfer, no swelling	(6)
		$\phi = 0.125$ in all cases	(7)
Ohtake et al. ¹¹	$d_{32}/d_1 = 0.12 We^{-0.5}$	$\mu_e < 0.16 \text{ N}\cdot\text{s}/\text{m}^2$, $\phi = 0.17$	(8)
	$d_{32}/d_1 = 0.002\mu_e \times 0.8 We^{-0.5}$	$\mu_e > 0.16 \text{ N}\cdot\text{s}/\text{m}^2$, $\phi = 0.17$	
		up to 30% swelling	
Sharma et al. ¹²	$\frac{d_{32}}{d_o} = (1 + BN_{Vi})^{0.6}$	$0.11 \text{ N}\cdot\text{s}/\text{m}^2 < \mu_e < 0.16 \text{ N}\cdot\text{s}/\text{m}^2$, Span 80, phenol	(9)
	$d_o = C_2(1 + a_1\Phi)^{1.2}(1 + a_2\phi)^{1.2} We^{-0.6} d_1$	transfer	(10)
	$N_{Vi} = \left(\frac{\rho_c}{\rho_d}\right)^{1/2} \frac{\mu_d \epsilon^{-1/3} d_{32}^{1/3}}{\sigma} (1 + a_1\Phi)^{-1} (1 + a_2\phi)^{-1}$	$\phi = 0.05, 0.025$; $\Phi = 0.32, 0.50, 0.58$	(11)

dilute dispersion no longer holds. However, the diversity of the equations reported in the literature indicates the difficulty of developing correlations of general validity. A recent publication by Zhou and Kresta⁴ presents a comprehensive updated review of d_{32} correlations. In an attempt to broaden the applicability of dispersion mean diameter correlations, Calabrese et al.^{5,6} and Wang and Calabrese⁷ conducted systematic studies on the dependency of equilibrium drop size and drop size distributions using a range of dispersed-phase viscosity of 0.1–10 N·s/m². A different behavior was observed for viscosity up to 0.5 N·s/m² as compared to high viscosities, with an erratic region between, confirming the importance of the dispersed-phase viscosity in the mechanisms of drop breakup and coalescence. In the range of viscosity up to 0.5 N·s/m², they also studied the effect of the dispersed-phase fraction⁶ and proposed a correction factor based on mechanistic arguments, which fits well their own and other authors' data.

Because dispersions are produced in order to generate an interfacial area for mass and/or heat transfer, the effect of these processes, particularly on interfacial tension and dispersed-phase viscosity, has to be incorporated in the correlations. In addition, it is no longer relevant to predict the drop sizes at dynamic equilibrium if the time scale for this is much larger than that for the transfer process equilibrium. Skelland and Lee⁸ studied dispersion accompanied by mass transfer at short contact times and developed an empirical correlation for the Sauter mean diameter that includes the Reynolds and the Ohnesorge numbers.

Emulsion dispersions are even more difficult to model because they are, in general, subjected to a number of nonidealities, such as emulsion swelling and rupture,⁹ and non-Newtonian behavior. On the other hand, both the presence of the surfactant in the membrane phase and the low dispersed-phase fraction required by the process make coalescence unlikely.

The few mean globule size correlations for emulsion dispersions found in the literature are summarized in Table 1 (eqs 4–11). The disparity of these equations reflects the scope of the problem, although there are some additional reasons that restrict a direct comparison. One is the diversity of techniques used for globule measurement and the relatively small number of globules measured. Another is that the phase selected to represent the effect of the dispersed-phase viscosity in data correlation is not the same. Kataoka and Nishiki¹⁰ used the membrane viscosity, i.e., the viscosity of the emulsion continuous phase, whereas Ohtake et al.¹¹ and Sharma et al.¹² used the viscosity of the emulsion, μ_e . Furthermore, Ohtake et al. reported emulsion non-

Newtonian behavior and took the value of μ_e at a shear rate of 10 s⁻¹; on the other hand, the emulsions studied by Sharma et al.¹² were Newtonian. Kataoka and Nishiki¹¹ obtained three different correlations, eqs 4–6 in Table 1, depending on the surfactant used to stabilize the emulsion, and in the case of the surfactant Span 80, a different equation was proposed for the case in which there was solute transfer. Emulsion swelling during solute extraction was observed in some of the emulsions. In the case of Span 80, they observed up to 30% emulsion swelling in the presence of solute transfer. The correlation proposed by Sharma et al.,¹² eqs 9–11 in Table 1, is based on those proposed by Calabrese et al.⁶ modified to account for the effect of both the encapsulated-phase volume fraction in the emulsion and the dispersed-phase volume fraction. None of the correlations in Table 1 include the effect of swelling as an independent parameter.

This review suggests that the relevant parameters for emulsion dispersion data correlation have not yet been completely identified. The present work examines the effect of emulsion swelling and shear-dependent emulsion viscosity on emulsion globule diameter, in addition to the usual correlating parameters. The experiments were conducted during the extraction of cadmium from and aqueous solution of phosphoric acid. The emulsion consisted of a NaCl solution encapsulated in a solution of the cadmium extractant Cyanex 302 in kerosene containing the surfactant Arlacel C as the emulsion stabilizer. The experiments were conducted in a stirred tank, and drop sizes were measured during the extraction of cadmium from the phosphoric acid phase from photographs taken with an endoscope attached to a high-speed video camera. Changes in the initial extractant and surfactant concentrations in the organic phase provided a wide range of emulsion viscosities and interfacial tensions between 0.0015 and 0.0020 N/m. The dispersed-phase ratio was varied between 0.025 and 0.070.

Experimental Section

All of the experiments were conducted at the continuous-phase initial concentration of 30 wt % P₂O₅ and 0.000 42 M CdSO₄. The organic phase of the water-in-oil emulsion was a solution of the extractant Cyanex 302 and the surfactant Arlacel C in low-odor kerosene. Arlacel C is the trademark name of a surfactant mixture whose main chemical component is sorbitan sesquiolate and was added to the organic phase in order to stabilize the emulsion. The effects of the initial concentrations of extractant and surfactant on the emulsion globule

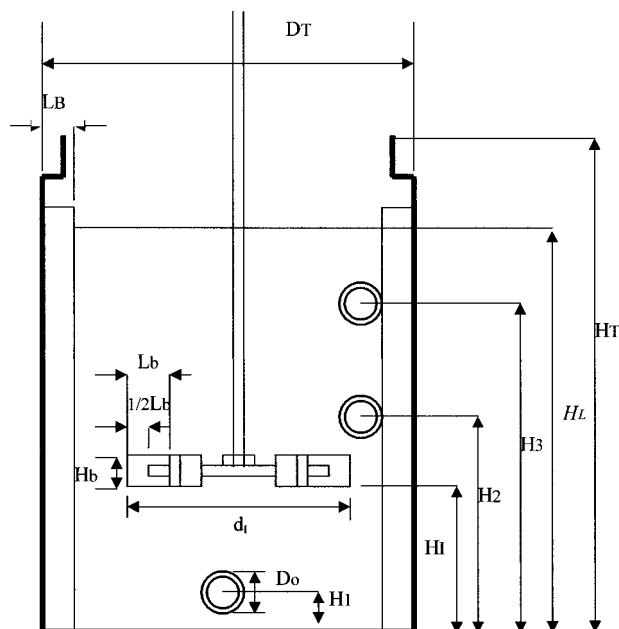


Figure 2. Tank configuration.

Table 2. Tank Dimensions^a

element	type/size (m)
internal diameter (D_T)	0.090
height (H_T)	0.132
liquid height (H_L)	0.125
impeller diameters (d_i)	0.036, 0.075, 0.085
type of impeller	flat blade turbine
no. of blades on the impeller	6
blade height (H_b)	0.006
height of the impeller off bottom (H_i)	0.113

^a Symbols from Figure 2.

size were investigated within an operative range established previously on the basis of the cadmium extraction performance.¹³ The lower value of the surfactant concentration, 3% (v/v), corresponds to the minimum value required to obtain a stable emulsion. The emulsion internal phase was an aqueous solution containing 3 M NaCl and 1 M HCl. The emulsion organic to aqueous phase ratio was 1:1. The emulsion formulation was selected from previous studies¹³ because of its stability and extraction performance and was prepared by adding the organic phase dropwise into the aqueous phase while stirring using a Silverson high-shear homogenizer at 3000 rpm. Once the dispersion was formed, cadmium was extracted into the emulsion organic phase by complexation with the extractant and stripped from there into the internal aqueous phase also by chemical reaction. The rate of cadmium extraction depended on extractant and surfactant concentrations and on the stirring speed.

Reagents. Cyanex 302 and Arlacel C were kindly supplied by Cytec Co. and by ICI Surfactants, respectively, $3\text{CdSO}_4 \cdot 8\text{H}_2\text{O}$ (99 wt %), H_3PO_4 (95 wt %), and the low-odor kerosene were purchased from Aldrich Chemical Co., and NaCl and HCl, both of analytical-grade quality, were obtained from Merck. All reagents were used without further purification.

Apparatus and Drop Sizing Technique. A schematic drawing of the cylindrical tank is shown in Figure 2, and its dimensions are listed in Table 2. The tank was fitted with sampling ports at two different heights to allow a 5 mm diameter endoscope to be placed inside

the dispersion. The endoscope was attached to a high-speed video camera system (Kodak Eckta Pro 1000 imager) and a high-powered light source. This setup allowed for pictures to be taken at up to 1000 frames/s while the dispersion was being stirred.

The resulting film was then digitized using the commercial software package Image-Pro Plus. This program enabled individual globules, displayed as dark circles, to be measured by the operator and the size to be recorded automatically. Drop size distributions and the Sauter mean diameter were obtained after measuring a total of over 1000 globules for each experimental condition. The Sauter mean diameter was calculated with eq 3.

Physical Properties. The physical and transport properties of the emulsion were measured at different extractant and surfactant concentrations. The initial composition of the continuous phase was the same in all runs. Globule sizes and physical properties of the emulsion were measured at a 10-min contact time with the aqueous phase; therefore, these measurements include the effect of cadmium extraction, emulsion swelling, and other phenomena associated with emulsion dispersion, such as secondary emulsification and rupture. The emulsion viscosity was determined at different shear rates with a Haake Rotovisco RV 100 Bohlin rotoviscometer, whereas the viscosity of the phosphoric acid solution was measured using a U-tube viscometer. Interfacial tensions were measured using a Krüss tensiometer with a de Noüy ring. All measurements were performed at $25 \pm 0.1^\circ\text{C}$.

Experimental Setup and Procedure. Runs were conducted at different extractant and surfactant concentrations and at various dispersed-phase fractions. Each experimental run was carried out in the following way:

- (1) An impeller size was selected.
- (2) The continuous and dispersed phases (note that in this paper the water-in-oil emulsion is referred as the dispersed phase) were prepared separately and placed in the tank at the selected emulsion initial volume fraction, ϕ^0 . The total initial volume was kept constant and equal to 750 mL. The impeller disk was always placed at a height of 0.113 m (Table 2), which placed the interface between the emulsion and the aqueous phase at the middle of the blade height for a holdup of 0.05. Although the range of holdups used in this paper was 0.025–0.067, the variation in the height of the interface was within the height of the blade (6 mm), so the impeller was always located at the interface between the emulsion and the continuous phase.
- (3) The impeller speed, N , was set, and stirring was started. All stirring speeds were above the minimum value for full dispersion.¹⁴
- (4) After a 10-min contact, photographs of the dispersion were taken. The amount of cadmium extracted during this time varied with the concentration of the extractant and surfactant, but at least 50% of the total extraction achieved at the end of the run (usually $t = 20$ min) was reached at $t = 10$ min.¹³
- (5) Recordings of drop size measurements were completed in the following 1.5 min and analyzed with the software package mentioned above.
- (6) The emulsion and continuous phases were separated, and the emulsion physical properties were measured.

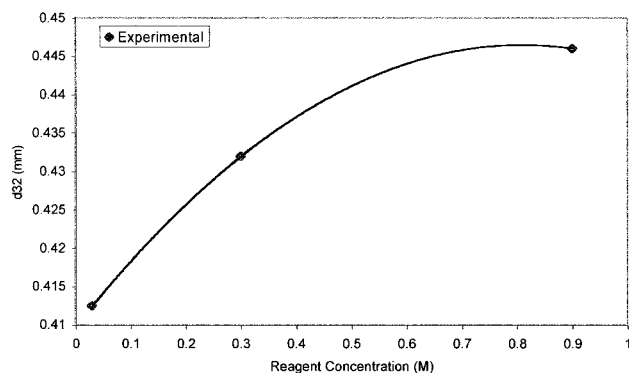


Figure 3. Effect of shear rate on the emulsion viscosity ([Arlacel C] = 5% (v/v), [Cyanex 302] = 0.3 M, $\Phi = 1$).

Table 3. Physical Properties of the Continuous^a and Dispersed Phases

[Cyanex 302] (M)	[Arlacel C] [% (v/v)]	σ_{e-c} (N/m)	ρ_e (kg/m ³)	μ_e^b (N·s/m ²)
0.03	5	1.5×10^{-3}	976.6	0.069
0.3	5	1.5×10^{-3}	980.2	0.101
0.3	1	2.0×10^{-3}	979.2	0.011
0.3	3	1.8×10^{-3}	979.7	0.042
0.3	10	1.5×10^{-3}	981.5	0.414
0.3	15	1.5×10^{-3}	982.7	0.421
0.9	5	1.5×10^{-3}	988.2	0.157

^a Continuous-phase properties: $\rho_c = 1360$ kg/m³, $\mu_c = 0.0046$ N·s/m². ^b At $\dot{\gamma} = 21$ s⁻¹.

Results and Discussion

Physical Properties of the Phases. The viscosity of the continuous phase and its density at 25 ± 0.1 °C were 0.0046 N·s/m² and 1360 kg/m³, respectively. The emulsion viscosity showed strong non-Newtonian behavior, as seen in Figure 3 where it is plotted vs shear rate for one of the emulsion formulations. The decrease of the viscosity was steep in the lower range of shear rates and reached a plateau at values above 230 s⁻¹. The same trend was observed in all of the investigated emulsion formulations. Results were well fit by

$$\mu_e \propto \dot{\gamma}^{-0.6} \quad (12)$$

which indicates that the behavior of the emulsion was pseudoplastic.

The effect of phase formulation on the emulsion physical properties is given in Table 3; in the case of viscosity, values were taken at an arbitrary value of $\dot{\gamma} = 21$ s⁻¹. It can be observed that the emulsion viscosity increased with both extractant and surfactant concentrations. It is interesting to note that the emulsion/continuous-phase viscosity ratio ranged approximately between 10 and 100. The density of the emulsion phase did not change much with formulation, with the average value being on the order of 980 kg/m³. The interfacial tension values listed in the table were measured in a two-phase system consisting of the continuous phase and an organic phase of the same composition as the emulsion organic phase. Results show that the interfacial tension was independent of the extractant concentration but decreased with the surfactant concentration, reaching a plateau at an Arlacel C concentration of 5%.

Emulsion Swelling and Rupture. The extraction process with a liquid membrane is generally accompanied by emulsion swelling either because of water formation by chemical reactions taking place at the

internal emulsion interface or because of water transfer through the organic phase of the emulsion, because surfactants used to stabilize the emulsions usually form reversed micelles. Swelling increases with contact time and may cause emulsion rupture, thus limiting the operational contact time. Another phenomenon caused by turbulent contact of the continuous and emulsion phases is emulsification of the continuous phase into the emulsion (secondary emulsification). It is not easy to decouple the effect of the different phenomena on emulsion volume or emulsion physical properties; therefore, in this work a net swelling factor was defined as the emulsion volume increase ratio

$$F^{Sw} = \Delta V_e / V_e^0 \quad (13)$$

where ΔV_e is the net change in the emulsion volume and V_e^0 is the initial emulsion volume. The increase in the emulsion volume at time t over the initial value is measured experimentally after stopping the stirrer. Values of the net swelling coefficients measured at a contact time of 10 min and at different operating conditions are given in Table 4. Swelling increased with the surfactant concentration, in agreement with data for some surfactants reported in the literature.^{15–17} However, it decreased with the reagent concentration, showing that there might be interactions between extractant and surfactant. Swelling also increased with the stirring speed, probably because of the larger specific interfacial area between the emulsion and the continuous phase and the higher mass-transfer coefficient in the phosphoric acid phase.

Hydrodynamic Conditions in the Tank. The stirring speed, N , and the impeller diameter, d_i , used in the different runs are listed in Table 4. Changes in either parameter alter both the power input per unit mass of dispersion and the local shear rates in the tank. Given that the dispersed-phase holdup is quite low, the profile of local velocity perturbations in the tank can be assumed to be determined by the Newtonian continuous phase. Measured values of the local average velocities in a tank of a similar configuration, reported by Cutter,¹⁸ show that the tangential velocity decreases with the radial distance from the impeller. In the region close to the impeller, the variation is at its maximum and is nearly linear. The equation

$$\dot{\gamma} = 2\pi N d_i / (d_T - d_i) \quad (14)$$

where d_T is the diameter of the tank, fits Cutter's results reasonably well up to a third of the distance between the tip of the impeller and the tank wall. The values of the shear rate in the region near the impeller for the different operating conditions calculated with eq 14 are given in Table 4.

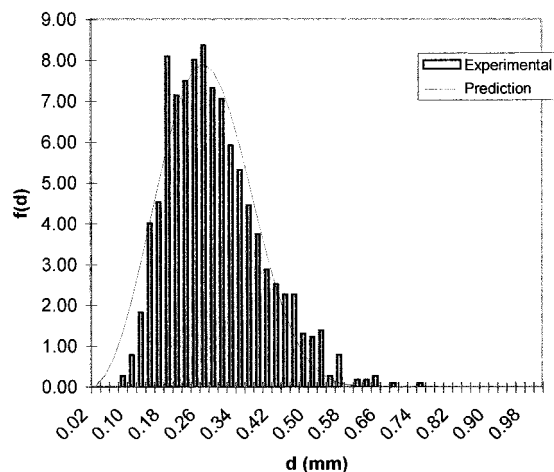
Also included in this table are the values of $N^3 d_i^2$. For conventional two-phase Newtonian dispersions, the power number N_{Ne} (also called the Newton number), defined as

$$N_{Ne} = P_M / N^3 d_i^2 \quad (15)$$

can be assumed to remain constant at Reynolds numbers greater than 10 000;¹⁹ therefore, in this region $N^3 d_i^2$ is proportional to the power input per unit mass. At $Re < 10$ 000, N_{Ne} increases with decreasing Re .

Table 4. Hydrodynamic Parameters in the Tank

[Cyanex 302] (M)	[Arlacel C] [% (v/v)]	d_t (mm)	N (rpm)	u_t (m/s)	$\dot{\gamma}$ (s ⁻¹)	$N^3 d_t^2$ (m ³ /s ²)	μ_e (N·s/m ²)	F^{Sw}
0.03	5	36	5.00	0.565	20.9	0.001 16	0.069	0.36
0.3	5	36	4.33	0.489	18.1	0.000 87	0.111	0.12
0.3	5	36	5.00	0.565	20.9	0.001 16	0.101	0.17
0.3	5	36	5.83	0.659	24.4	0.001 58	0.092	0.25
0.3	5	36	6.67	0.754	27.9	0.002 07	0.088	0.33
0.3	5	75	5.00	1.178	78.5	0.010 54	0.052	0.17
0.3	5	85	5.00	1.335	267	0.015 35	0.034	0.17
0.6	5	36	5.00	0.565	20.9	0.001 16		0.12
0.9	5	36	5.00	0.565	20.9	0.001 16	0.157	0.02

**Figure 4.** Comparison of experimental and drop size distribution by a modified Rosin–Rammler distribution model with experimental results ([Arlacel C] = 5% (v/v), [Cyanex 302] = 0.3 M, N = 4.16 rpm, d_t = 0.036 m).**Table 5. Globule Size Distribution Coefficients for Different Surfactant Concentrations**

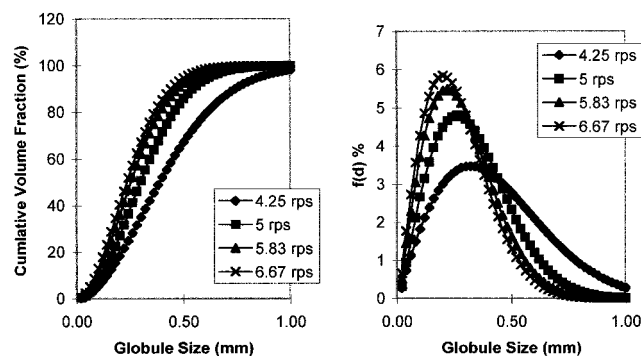
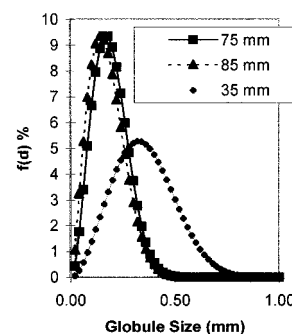
[Cyanex 302] (M)	[Arlacel C] [% (v/v)]	d_t (mm)	N (s ⁻¹)	ϕ	x	w
0.3	5	36	6.67	0.05	0.8542	2.599
0.3	5	36	5.83	0.05	0.8958	2.887
0.3	5	36	4.58	0.05	0.8321	2.436
0.3	5	36	4.25	0.05	0.8817	2.545
0.3	3	36	5	0.067	0.7123	0.854
0.3	3	36	5	0.033	0.7124	1.898
0.3	3	36	5	0.025	0.7530	1.382
0.3	5	75	5	0.05	0.8740	2.336
0.3	5	85	5	0.05	0.8769	2.037
0.3	5	36	5	0.05	0.8578	2.593
0.3	3	36	5	0.05	0.8545	1.913
0.3	1	36	5	0.05	0.8553	1.752

Globule Size Distribution. Figure 4 displays a typical drop size distribution. The cumulative volume fraction of globules below a given size d_t , was well described by the modified Rosin–Rammler²⁰ distribution model given by the expression

$$P(d_t < d) = [1 - \exp(-x(d/d_{12})^w)] \quad (16)$$

where d_{12} is the arithmetic mean drop size calculated from globule size measurements and x and w are parameters that vary with surfactant and reactant compositions and operating conditions. The continuous curve shown in Figure 4 was obtained with eq 16. Optimum values of x and w used to fit this distribution to the experimental data are given in Table 5.

Figure 5 shows drop size distributions obtained for an emulsion liquid membrane containing 0.3 M Cyanex 302 and 5% (v/v) surfactant Arlacel C, at four rotating speeds. As the rotation speed increased, the distribution

**Figure 5.** (a) Fitted cumulative distribution. (b) Fitted drop size distribution. Effect of stirring speed on globule size distribution and cumulative size distribution ([Cyanex 302] = 0.3 M, [Arlacel C] = 5% (v/v), Φ = 0.05, d_t = 0.036 m).**Figure 6.** Effect of impeller diameter on the drop size distribution (Φ = 0.05, N = 5 rpm, [Cyanex 302] = 0.3 M).

became skewed and shifted to smaller sizes and the peak became higher, in a way similar to that in some conventional two-phase dispersions.²¹ Increasing the impeller diameter led to an analogous effect, as seen in Figure 6. This was expected because the increase in either N or d_t produced an increase in P_M (Table 4), which in turn would lead to smaller drop sizes.

Sauter Mean Diameter Data. The Sauter mean diameters were calculated with eq 3. The analysis of the dependency of d_{32} on the hydrodynamic parameters and the physical properties is complicated by the fact that they are not independent parameters, as can be seen in Tables 3 and 4. Modifications to the emulsion composition carried out to change the emulsion viscosity were accompanied by changes in interfacial tension and swelling. Not even N was an independent parameter because it changed the swelling factor (Table 4) and the viscosity of the deforming emulsion globule, as discussed later. However, these are characteristics of the system that cannot be eliminated without changing the system. The analysis presented in the following sections is an attempt to decouple the effect of the different parameters and assess their relative importance in the mechanism of globule breakup.

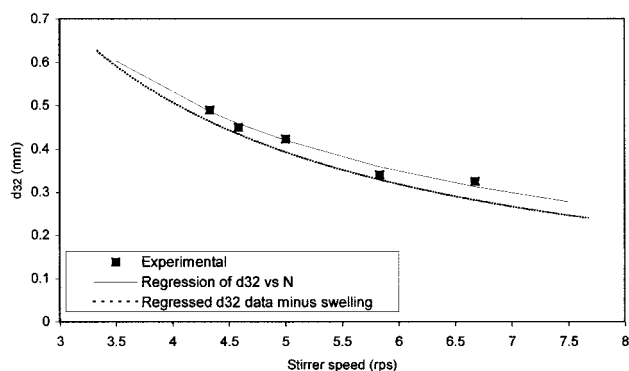


Figure 7. Effect of stirring speed on the globule Sauter mean diameter ([Arlacel C] = 5% (v/v), [Cyanex 302] = 0.3 M, $\Phi = 0.05$, $d_t = 0.036$ m).

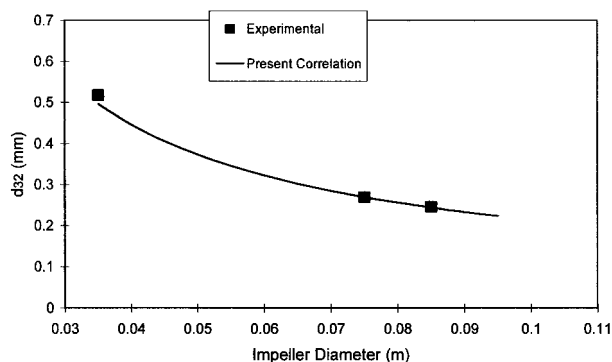


Figure 8. Effect of impeller diameter on the globule Sauter mean diameter ([Arlacel C] = 5% (v/v), [Cyanex 302] = 0.3 M, $\Phi = 0.05$, $N_{\text{stirrer}} = 4.25$ rps).

(a) Effect of the Stirring Speed, Impeller Diameter, and Dispersed-Phase Fraction. Figure 7 shows the variation of the Sauter mean diameter with stirring speed for an emulsion with a membrane phase containing 0.3 M Cyanex 302 and 5% (v/v) Arlacel C and an initial dispersed-phase volume fraction, ϕ^0 , of 0.05. Regression of the experimental data obtained from these experiments, and from those performed using an emulsion containing 3% Arlacel C (not shown in the figure for clarity), gave a dependency of the globule Sauter mean diameter on the stirring speed of $d_{32} \propto N^{-1.03}$. In absolute value, this power is below -1.2 , which is the one given by theoretical predictions for dilute Newtonian dispersions subjected to isotropic turbulence¹ and approximately the same as that obtained by Ohtake et al. (eqs 7 and 8 in Table 1). When swelling was subtracted from the d_{32} values using the coefficients listed in Table 4, the slope of the curve increased, as shown also in Figure 7, and the curve was well fitted by $d_{32} \propto N^{-1.12}$, which is closer to the dependency given by eq 1.

The variation of d_{32} with the impeller size at the same stirring speed is displayed in Figure 8. The Sauter mean diameter decreased with increasing d_t , as expected, because of the increase in P_M . The dependency of the mean globule diameter on the impeller size was well fitted by $d_{32} \propto d_t^{-0.84}$.

Shown in Figure 9 is the plot of d_{32} vs ϕ^0 for an emulsion containing 0.3 M Cyanex 302 and 5% (v/v) Arlacel C. A weak effect of the dispersed-phase fraction, ϕ^0 , on d_{32} was observed at all conditions investigated, suggesting that the combined effect of the low dispersed-phase holdup and of the presence of the surfactant hindered globule coalescence.

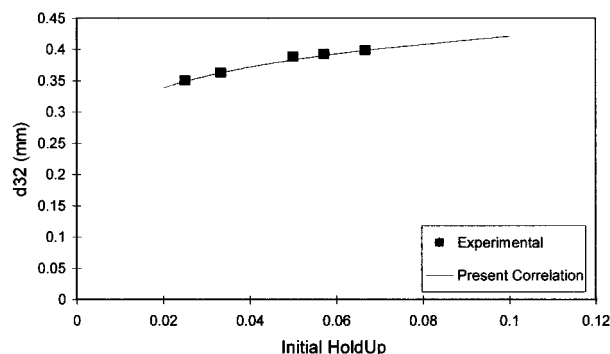


Figure 9. Effect of holdup on the globule Sauter mean diameter ([Arlacel C] = 5% (v/v), [Cyanex 302] = 0.3 M, $N_{\text{stirrer}} = 6.67$ rps, $d_t = 0.036$ m).

(b) Effect of the Emulsion Viscosity, Interfacial Tension, and Swelling. The few correlations for the Sauter mean diameter of emulsion globules reported in the literature^{11,12} involve the emulsion viscosity as one of the independent parameters; the effect of the dispersed-phase viscosity has also been included in correlations for conventional two-phase dispersions.^{5,22–24} If the emulsion viscosity is assumed to be important as a resistive force in the mechanism of globule breakup, then it is its effective value during globule breakage that will be the key parameter for drop size correlation. Although the presence of the surfactant is expected to prevent internal circulation, globule deformation due to local turbulence will generate internal flows and therefore shear rates whose magnitude will depend on the rate of globule deformation. If the latter is assumed to increase with turbulence intensity, then the viscosity of a breaking globule would be related to the local turbulence intensity in the continuous phase. Given that the surfactant is likely to prevent globule coalescence, drop breakup is likely to occur mainly in the impeller region, because this is the area of highest turbulence. Therefore, as a first approximation, the values of the operational viscosity were taken at the estimated shear rates in this region calculated with eq 14. These are listed in Table 4.

Varying between 0.034 and 0.157 N·s/m², the emulsion operational viscosity was the parameter with the widest variation range, as seen in Table 4. Emulsion viscosity changed not only with the hydrodynamic conditions but also with the surfactant and extractant concentrations; therefore, its effect on mean globule diameter cannot be easily decoupled from those of interfacial tension and swelling, which change with the same parameters in a diverse way. Parts a–c of Figure 10 show plots of d_{32} vs the concentration of Arlacel C, together with the corresponding values of the interfacial tension, swelling, and emulsion viscosity at a constant stirring speed of 5 rps. In the range of concentration up to 5%, the interfacial tension decreased with the surfactant concentration, whereas the emulsion viscosity and swelling increased and the Sauter mean diameter remained approximately constant. Thus, as one of the forces resisting breakup decreased (the interfacial tension), the other one (viscosity) increased, which together with higher swelling would cancel the effect of the interfacial tension. Above 5% (v/v) Arlacel C concentration, the interfacial tension remained constant and both the viscosity and swelling continued increasing with the surfactant concentration, and so did d_{32} . These results do not allow an assessment of the relative effect

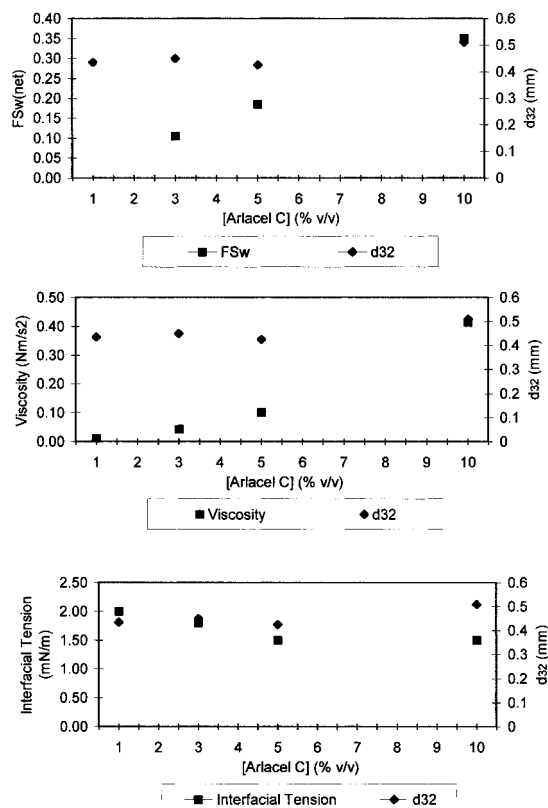


Figure 10. Effect of Arlacel C concentration on the globule Sauter mean diameter, net swelling, emulsion viscosity, and interfacial tension between the emulsion and continuous phases ([Arlacel C] = 5% (v/v), $\Phi = 0.05$, $N_{\text{stirrer}} = 5$ rps, $d_1 = 0.036$ m).

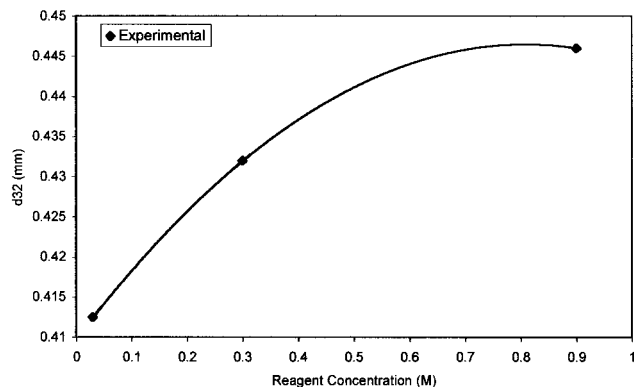


Figure 11. Effect of Cyanex 302 concentration on the globule Sauter mean diameter ([Arlacel C] = 5% (v/v), $\Phi = 0.05$, $N_{\text{stirrer}} = 5$ rps, $d_1 = 0.036$ m).

of the emulsion viscosity and swelling on the resulting globule mean size. A possibility of decoupling the effects of viscosity and swelling is to examine the effect of the concentration of Cyanex 302 on d_{32} at constant surfactant concentration, because the viscosity increased with the extractant concentration, whereas swelling decreased (Tables 3 and 4). Results plotted in Figure 11 show that d_{32} increased with the extractant concentration. This indicated that the effect of viscosity was predominant in this range of conditions, and therefore it could not be neglected as a correlation parameter.

Sauter Mean Diameter Correlation. The experimental data suggested that swelling was the main phenomenon responsible for the deviations of the globule size dependency on We predicted by eq 1, with a minor influence from both μ_e and ϕ^0 . Therefore, a

predictive equation was developed that included these parameters.

It was assumed that globule coalescence was negligible because of the presence of the surfactant and the low emulsion holdup and that globules first formed and then swelled. For spherical globules, the change in the Sauter mean diameter due to net swelling can be calculated from the emulsion net swelling factor F^{sw} (eq 13) as

$$F^{\text{sw}} = \frac{d_{32}^3 - (d_{32}^0)^3}{(d_{32}^0)^3} \quad (17)$$

or

$$d_{32} = d_{32}^0 (1 + F^{\text{sw}})^{1/3} \quad (18)$$

where d_{32}^0 is the globule Sauter mean diameter before swelling, corrected empirically for ϕ^0 and μ_e as suggested by the analysis of the data. It was further assumed that d_{32}^0 could be calculated from eq 1, empirically corrected for the effects of the emulsion viscosity and of the dispersed-phase fraction:

$$d_{32}^0/d_1 = C_3 We^{-0.6} (\phi^0)^a (\mu_e/\mu_c)^b \quad (19)$$

Combining eqs 18 and 19 yields

$$d_{32}/d_1 = C_3 We^{-0.6} (\phi^0)^a (\mu_e/\mu_c)^b [1 + F^{\text{sw}}]^{1/3} \quad (20)$$

The optimized values for the three constants are $C_3 = 0.75$, $a = 0.136$, and $b = 0.11$. The small values for a and b reflect the weak effect of holdup and emulsion viscosity on mean globule size, leaving power input and net swelling as the main mechanisms that affect globule size. However, it must be remembered that swelling and μ_e are not independent parameters, because they depend not only on each other but also on ϕ^0 and N . Therefore, the swelling correction factor implicitly includes the influence of the other parameters. Thus it could be quite a useful correlating parameter given that emulsion swelling is easy to measure. Experimental results on swelling²⁵ indicate that for a given emulsion formulation the swelling factor is independent of the water mass-transfer coefficient in the phosphoric acid phase and, within the experimental error, proportional to the globule interfacial area. Therefore, if the scale-up factor for equal d_{32} is constant power input per unit mass, which is implicit when using $We^{-0.6}$, then the swelling factor measured in a small tank should be the same for a bigger tank of the same configuration. However, the suitability of the equal power input rule to scale-up the emulsion dispersion should be first tested, because it is not always applicable even to conventional two-phase dispersions.²¹

The absolute value of the average relative error percentage, AARE (%), defined as

$$\text{AARE (\%)} = \frac{|d_{32}^{\text{predicted}} - d_{32}^{\text{experimental}}|}{d_{32}^{\text{experimental}}} \times 100 \quad (21)$$

for eq 20 was 4.90. The fit of this correlation to the data is shown in Figure 12. The ratio of maximum stable globule size to Sauter mean diameter constant for all the data of this study is 2.1 ± 0.40 .

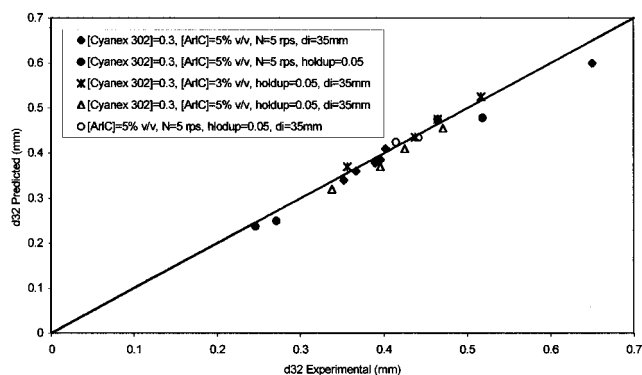


Figure 12. Goodness of predictions.

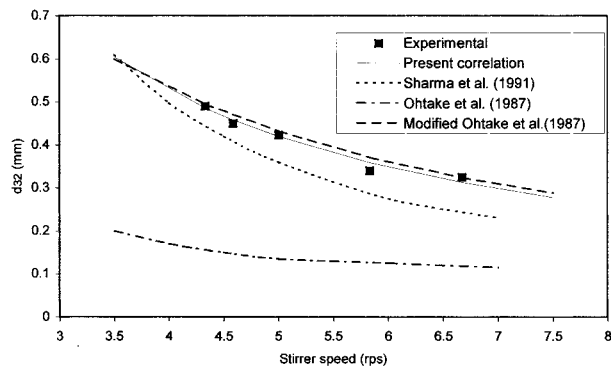


Figure 13. Effect of stirring speed on the globule Sauter mean diameter: comparison of correlations.

(a) Comparison of Correlations. The fits of the correlations by Ohtake et al.¹¹ and by Sharma et al.¹² are shown in Figure 13. Although the correlation of Ohtake and co-workers for $\mu_e < 0.16 \text{ N}\cdot\text{s}/\text{m}^2$ (eq 7) underestimates d_{32} , it is not surprising that it predicts the trend of the data well, because it contains $We^{-0.5}$, which is the same dependency on We as in the correlation proposed here. It should be noted that eq 7 was developed for emulsions with levels of swelling similar to those of the data reported here. Changing the constant in eq 7 to the value 0.38 gives a good fit to the data obtained in this work. Equation 9¹² also underestimates the mean globule size, and furthermore it does not predict well the trend of the data.

The lack of agreement between the d_{32} values calculated from different correlations is not surprising because the dispersions from which they were developed had diverse characteristics and physical properties: some of the emulsions were Newtonian, some showed swelling, and some were investigated during mass transfer. Therefore, these studies, including the present one, are primarily aimed at assessing the scope of the problem and identifying the relevant parameters for data correlation.

Conclusions

The emulsion shear-dependent viscosity, swelling, dispersed-phase holdup, and operating conditions are interrelated in such a complex way that they did not allow for a mechanistic approach to globule size prediction. However, emulsion swelling seemed to lump together the effect of some of the parameters on globule size and made possible the development of a simple correlation for the Sauter mean diameter in terms of $We^{-0.6}$, emulsion swelling percentage, and empirical correction factors for emulsion viscosity and dispersed-

phase holdup. The equation fitted well the experimental data within an absolute value of the average relative error of 4.90%. A modified Rosin–Rammler probability distribution fitted well the globule size distribution data.

Acknowledgment

Financial support from the European Union is gratefully acknowledged. We also thank Cytec Industries and ICI Surfactants for providing the reagent and surfactant used in this work and Dr. J. Stoyel for his advice on the use of the drop measuring technique. The authors wish to thank the referees for their constructive remarks.

Nomenclature

- a, b = constants
- a_1, a_2 = turbulence damping constant
- B = constant
- C_1 – C_3 = constants
- D_o = outlet diameter, m
- D_T, d_T = tank diameter, m
- d_{12} = arithmetic mean globule diameter, m
- d_{32} = Sauter mean globule diameter, m
- d_{32}^0 = Sauter mean globule diameter at substantially zero swelling, m
- d_i = globule diameter, m
- d_i = impeller diameter, m
- F^{Sw} = swelling correction factor
- H = height of the vessel, m
- H_b = height of the blade, m
- L_b = length of the blade, m
- N = impeller speed, rps
- n_i = number of globules
- N_{Ne} = Newton number
- N_{vi} = viscosity number
- P_M = power dissipated by the impeller per unit mass, m^2/s^3
- Re = Reynolds number, defined as $Re = Nd_i^2\rho_c/\mu_c$
- V_i = volume of phase i , m^3
- ΔV_i = absolute difference in volume of phase i , m^3
- We = Weber number, defined as $We = N^2 d_i^3 \rho_c / \sigma$
- w = globule size distribution coefficient
- x = globule size distribution coefficient
- $[]$ = concentration, M or % v/v

Greek Symbols

- ϵ = mechanical power dissipation per unit mass, W/kg
- ϕ = volume fraction of the ELM dispersed phase (V_e/V_i)
- Φ = dispersed phase volume fraction in the emulsion (V_3/V_2)
- $\dot{\gamma}$ = shear rate, s^{-1}
- μ = viscosity, $\text{N}\cdot\text{s}/\text{m}^2$
- ρ = density, kg/m^3
- σ = interfacial tension, N/m

Subscripts

- 1 = ELM continuous phase
- 2 = ELM membrane phase
- 3 = ELM stripping phase
- c = continuous phase
- e = emulsion phase

Superscripts

- 0 = at initial conditions
- Sw = due to swelling
- t = at given time t

Literature Cited

- (1) Hinze, J. O. Fundamentals of the Hydrodynamic Mechanism of Splitting in Dispersion Processes. *AIChE J.* **1955**, *1*, 289.
- (2) Shinnar, R.; Church, J. M. Statistical Theories of Turbulence in Predicting Particle Size in Agitation Dispersions. *Ind. Eng. Chem.* **1960**, *52*, 253.
- (3) Kolmogorov, A. V. The Breakup of Droplets in a Turbulent Stream. *Dokl. Akad. Nauk.* **1949**, *66*, 825.
- (4) Zhou, G. W.; Kresta, S. M. Correlation of Mean Drop Size and Minimum Drop Size with the Turbulence Energy Dissipation and the Flow in an Agitated Tank. *Chem. Eng. Sci.* **1998**, *53*, 2063.
- (5) Calabrese, R. V.; Chang, T. P.; Dang, P. T. Drop Breakup in Turbulent Stirred Tank Contactors. Part I: Effect of Dispersed-Phase Viscosity. *AIChE J.* **1986**, *32*, 657.
- (6) Calabrese, R. V.; Wang, C. Y.; Bryner, N. P. Drop Breakup in Turbulent Stirred Tank Contactors. Part III: Correlations for Mean Size and Drop Size Distributions. *AIChE J.* **1986**, *32*, 677.
- (7) Wang, C. Y.; Calabrese, R. V. Drop Breakup in Turbulent Stirred-Tank Contactors. Part II: Relative Influence of Viscosity and Interfacial Tension. *AIChE J.* **1986**, *32*, 667.
- (8) Skelland, A. H. P.; Lee, J. M. Drop Size and Continuous Phase Mass Transfer in Agitated Vessels. *AIChE J.* **1981**, *27* (1), 99.
- (9) Itoh, H.; Thien, M. P.; Hatton, T. A.; Wang, D. I. C. Water Transport Mechanism in Liquid Emulsion Membrane Process for the Separation of Amino Acids. *J. Membr. Sci.* **1990**, *51*, 309.
- (10) Kataoka, T.; Nishiki, T. Dispersed Mean Drop Sizes of (W/O)/O Emulsions in a Stirred Tank. *J. Chem. Eng. Jpn.* **1986**, *19*, 408.
- (11) Ohtake, T.; Hano, T.; Takagi, K.; Nakashio, F. Effects of Viscosity on Drop Diameter of W/O Emulsion Dispersed in a Stirred Tank. *J. Chem. Eng. Jpn.* **1987**, *20*, 443.
- (12) Sharma, A.; Goswami, A. N.; Rawat, B. S. Drop Size Prediction in Liquid Membrane Systems. *J. Membr. Sci.* **1991**, *60*, 261.
- (13) Gallego-Lizon, T.; Pérez de Ortiz, E. S. Separation of Cadmium from Phosphoric acid containing Cu^{2+} and Cd^{2+} Using Surfactant Liquid Membranes. In *International Symposium on Liquid-Liquid Two-Phase Flow and Transport and Phenomena*; Maron, D. M., Ed.; Begell House: New York, 1997; p 301.
- (14) Skelland, A. H. P.; Lee, J. M. Agitator Speeds in Baffled Vessels for Uniform Liquid-Liquid Dispersions. *Ind. Eng. Chem., Process Des. Dev.* **1978**, *17* (4), 473.
- (15) Mok, Y. S.; Lee, W. K. Water Transport in Water-in-Oil-in-Water Liquid Emulsion Membrane Systems for the Separation of Lactic Acid. *Sep. Sci. Technol.* **1994**, *29*, 743.
- (16) Mok, Y. S.; Lee, K. H.; Lee, W. K. Control of Swelling in Liquid Emulsion Membranes Employed for Lactic Acid Separation. *J. Chem. Technol. Biotechnol.* **1996**, *65*, 309.
- (17) Shen, J. Q.; Yin, W. P.; Zhao, Y. Y.; Yu, L. J. Extraction of Alanine Using Emulsion Liquid Membranes Featuring a Cationic Carrier. *J. Membr. Sci.* **1996**, *120*, 45.
- (18) Cutter, L. A. Flow and Turbulence in a Stirred Tank. *AIChE J.* **1966**, *12*, 35.
- (19) Rushton, J. H.; Costich, E. W.; Everett, H. J. Power Characteristics of Mixing Impellers, Part I. *Chem. Eng. Prog.* **1950**, *46*, 395.
- (20) Rosin, P.; Rammner, E. The Laws Governing the Fineness of Powdered Coal. *Inst. Fuel J.* **1933**, *82*, 29.
- (21) Okufi, S.; Pérez de Ortiz, E. S.; Sawistowski, H. Scale-up of Liquid-Liquid Dispersions in Stirred Tanks. *Can. J. Chem. Eng.* **1990**, *68*, 400.
- (22) Doulah, M. S. An Effect of Hold-up on Drop-Size in Liquid-Liquid Dispersions. *Ind. Eng. Chem. Fundam.* **1975**, *14*, 137.
- (23) Tong, J.; Furusaki, S. Mean Drop Size and Size Distribution in a Rotating Disc Contactor Used for Reversed Micellar Extraction of Proteins. *J. Chem. Eng. Jpn.* **1995**, *28*, 582.
- (24) Kuriyama, M.; Ono, M.; Tokanai, H.; Konno, H. Correlation of Transient Sizes of Highly Viscous Drops in Dispersion Processes in Liquid-Liquid Agitation. *Chem. Eng. Res. Des.* **1996**, *74*, 431.
- (25) Gallego-Lizon, T. Cadmium Separation from Phosphoric Acid Using the Emulsion Liquid Membrane. Ph.D. Dissertation, University of London, U.K., 1998.

Received for review January 3, 2000

Revised manuscript received August 15, 2000

Accepted September 13, 2000

IE000016Y